Structural and Dynamic Properties of the Homodimeric Hemoglobin from Scapharca inaequivalvis Thr−72→Ile Mutant: Molecular Dynamics Simulation, Low Temperature Visible Absorption Sp…

ARTICLE *in* BIOPHYSICAL JOURNAL · NOVEMBER 1998

Impact Factor: 3.97 · DOI: 10.1016/S0006-3495(98)77693-3 · Source: PubMed

9 AUTHORS, INCLUDING:

Alessandro Desideri
University of Rome Tor Vergata
313 PUBLICATIONS **4,514** CITATIONS
SEE PROFILE

Maurizio Leone
Università degli Studi di Palermo
154 PUBLICATIONS **2,411** CITATIONS
SEE PROFILE

Joel M Friedman
Albert Einstein College of Medicine
256 PUBLICATIONS **7,892** CITATIONS
SEE PROFILE

Alessandra Gambacurta
University of Rome Tor Vergata
30 PUBLICATIONS **240** CITATIONS
SEE PROFILE

Structural and Dynamic Properties of the Homodimeric Hemoglobin from *Scapharca inaequivalvis* Thr-72→Ile Mutant: Molecular Dynamics Simulation, Low Temperature Visible Absorption Spectroscopy, and Resonance Raman Spectroscopy Studies

Mattia Falconi,* Alessandro Desideri,* Antonio Cupane,# Maurizio Leone,# Giovanni Ciccotti,§ Eric S. Peterson,¶ Joel M. Friedman,¶ Alessandra Gambacurta,‖ and Franca Ascoli‖

*Department of Biology and INFM, University of Rome "Tor Vergata," 00133 Roma, Italy; #Institute of Physics and INFM, University of Palermo, 90123 Palermo, Italy; §Department of Physics and INFM, University of Rome "La Sapienza," 00100 Roma, Italy; ¶Albert Einstein College of Medicine, Department of Physiology and Biophysics, Bronx, New York 10461 USA; and ‖Department of Experimental Medicine and Biochemical Sciences, University of Rome "Tor Vergata," 00133 Roma, Italy

ABSTRACT Molecular dynamics simulations, low temperature visible absorption spectroscopy, and resonance Raman spectroscopy have been performed on a mutant of the *Scapharca inaequivalvis* homodimeric hemoglobin, where residue threonine 72, at the subunit interface, has been substituted by isoleucine. Molecular dynamics simulation indicates that in the Thr-72→Ile mutant several residues that have been shown to play a role in ligand binding fluctuate around orientations and distances similar to those observed in the x-ray structure of the CO derivative of the native hemoglobin, although the overall structure remains in the T state. Visible absorption spectroscopy data indicate that in the deoxy form the Soret band is less asymmetric in the mutant than in the native protein, suggesting a more planar heme structure; moreover, these data suggest a similar heme-solvent interaction in both the liganded and unliganded states of the mutant protein, at variance with that observed in the native protein. The "conformation sensitive" band III of the deoxy mutant protein is shifted to lower energy by >100 cm^{-1} with respect to the native one, about one-half of that observed in the low temperature photoproducts of both proteins, indicating a less polar or more hydrophobic heme environment. Resonance Raman spectroscopy data show a slight shift of the iron-proximal histidine stretching mode of the deoxy mutant toward lower frequency with respect to the native protein, which can be interpreted in terms of either a change in packing of the phenyl ring of Phe-97, as also observed from the simulation, or a loss of water in the heme pocket. In line with this latter interpretation, the number of water molecules that dynamically enters the intersubunit interface, as calculated by the molecular dynamics simulation, is lower in the mutant than in the native protein. The 10-ns photoproduct for the carbonmonoxy mutant derivative has a higher iron-proximal histidine stretching frequency than does the native protein. This suggests a subnanosecond relaxation that is slowed in the mutant, consistent with a stabilization of the R structure. Taken together, the molecular dynamics and the spectroscopic data indicate that the higher oxygen affinity displayed by the Thr-72→Ile mutant is mainly due to a local perturbation in the dimer interface that propagates to the heme region, perturbing the polarity of the heme environment and propionate interactions. These changes are consistent with a destabilization of the T state and a stabilization of the R state in the mutant relative to the native protein.

INTRODUCTION

The homodimeric hemoglobin (HbI) from the bivalve mollusk *Scapharca inaequivalvis* binds oxygen with constant oxygen affinity in the pH range 5–9, a significant cooperativity with a Hill coefficient of 1.5 and a free energy of interaction of ~1 kcal/mol per site (Chiancone et al., 1981; Ikeda-Saito et al., 1983). The protein has been the subject of several functional and structural investigations showing that cooperativity in this protein is based on a direct communication between the two heme groups that results from a unique assembly of the globin chains (Royer et al., 1990). The x-ray structure of both the liganded and unliganded forms of the protein has recently been solved at high resolution (Royer, 1994). This study indicates that the intersubunit interface is made by the heme-carrying E and F helices and that Phe-97 plays a crucial role in modulating the oxygen affinity of this protein. In particular, Phe-97 is extruded toward the subunit interface upon ligand binding and makes close hydrophobic interaction with the Thr-72 residue of the other subunit. Because of the packing of Phe-97 at the interface and because of the occurrence of a short hydrogen bond between the carbonyl of Phe-97 and the Nδ1 of the proximal histidine it was proposed that this residue plays a primary role in modulating the oxygen binding properties of the protein (Royer, 1994).

On the basis of these considerations a Thr-72→Ile mutant has recently been expressed that aims to increase the hydrophobic character of the interface; such a mutant was actually found to highly enhance oxygen affinity and markedly reduce cooperativity (Gambacurta et al., 1995).

In an attempt to understand the structural dynamics difference between the mutant and the wild type that gives rise

Received for publication 27 April 1998 and in final form 6 July 1998.

Address reprint requests to Dr. Alessandro Desideri, Department of Biology, University of Rome "Tor Vergata," Via della Ricerca Scientifica, 00133 Roma, Italy. Tel.: +39-06-72594376; Fax: +39-06-72594311; E-mail: desideri@uniroma2.it.

0006-3495/98/11/2489/15 $2.00

to such oxygen binding differences, a molecular dynamics (MD), a low temperature visible absorption, and a resonance Raman study has been carried out. The choice of these different techniques relies on the fact that they are complementary. MD may in fact accurately probe the structural dynamics properties of all the residues, but is less sensitive in monitoring the heme motions because of the constraints used in the potential parameters for the heme (Kuczera et al., 1990). At difference, low temperature optical spectroscopy has been shown to be particularly sensitive to the movements of the iron with respect to the heme plane (Melchers et al., 1996; Leone et al., 1994); the temperature dependence of the optical absorption spectra may in fact give information on the stereodynamic properties of the active site by taking advantage of the fact that the lineshape of the Soret band is influenced by the coupling of the electronic transition with the vibrational modes of the matrix surrounding the chromophore, as well as by homogeneous and inhomogeneous broadening. Such an approach has been used to describe the structural dynamics properties of several metalloproteins in considerable detail (Cupane et al., 1994–1996) and has been successfully applied to investigate the properties of native HbI (Boffi et al., 1994). The thermal behavior of the near-infrared band III, originating from a porphyrin to iron charge transfer transition, has also been investigated since this band has been shown to probe the local structure of the heme within the heme pocket (Sassaroli and Rousseau, 1987; Chavez et al., 1990; Gilch et al., 1996) and to be sensitive to electrostatic and hydrophobic effects that usually cannot be detected even by high resolution x-ray diffraction studies. However, resonance Raman spectroscopy in the frequency region 180–400 cm^{-1} is a sensitive probe of the iron–proximal histidine linkage as well as of the heme pocket conformation of *S. inaequivalvis* HbI (Song et al., 1993; Rousseau et al., 1993).

Because the results from MD studies on proteins are significantly influenced by solvent effects (Dagget and Levitt, 1993), the simulations have been performed in an aqueous environment. Comparison of the trajectories observed for the mutant and the native deoxygenated proteins indicate a different dynamic behavior that may explain the different oxygen affinity in the two proteins. In particular, it appears that although the overall quaternary structure remains in the T state, several functionally important residues gain access in the deoxy derivative configurations similar to those observed in the HbI-CO. Consistently, the spectroscopic data suggest a stabilization of the R structure and a similar heme-solvent interaction in both the liganded and unliganded states of the mutant protein.

Taken together, the results worked out from both the MD simulations and the spectroscopic data indicate that the higher oxygen affinity displayed by the Thr-72→Ile mutant is due to small local perturbations in the hydrogen bonding pattern of the dimer interface, which destabilize the T state and stabilize the R state.

MATERIALS AND METHODS

Molecular modeling

The mutant and the wild-type proteins have been modeled by using the computer program Sybyl V6.0 by Tripos Associates (St. Louis, MO). The interface residue Thr-72 has been changed in isoleucine conserving the atomic positions of the Cβ and Cγ atoms of the branched threonine side chain. Because of the use of the united atom approximation (Brooks et al., 1983), the substitution of the threonine hydroxyl group by an isoleucine butyl group does not modify the total number of protein atoms. After changing the side-chain atoms, the isoleucine 72 residue has been checked against contacts with the other interface residues. The side chain of the substituted residue Ile-72 is easily accommodated in the space between the E and F helices of each subunit. Since in the original crystallographic Protein Data Bank (Bernstein et al., 1977) file (entry 4sdh) the first residue of Pre-A helix Pro-1 is missing, it has been added in both the wild-type and mutant protein.

Molecular dynamics

The molecular dynamics simulation has been performed using the computer program ORAC (Procacci et al., 1997). The coordinates of the *S. inaequivalvis* deoxy homodimer at 1.6 Å resolution (Royer, 1994) were obtained from the Brookhaven Protein Data Bank (Bernstein et al., 1977). A rectangular box with volume of $\sim 58 \times 58 \times 58$ $Å^3$ was generated by translation of a primitive simple cubic cell containing a water molecule to give a molecular lattice with the density of 1 gr/cm^3 at 300 K. The protein, in the x-ray configuration with its 219 crystal waters, has been inserted in the center of the water-filled simulation box. Only solvent molecules whose atoms were >90% the sum of the corresponding Lennard-Jones radii away from solute and crystallographic water atoms were kept. With the remaining 4502 water molecules, the protein concentration was 8.2 mM. Four water molecules, chosen far enough from the protein salt bridges, were replaced by chloride ions to make the system electroneutral. The system thus consisted of 16,368 atoms, of which 2858 were the protein itself, 13,506 of the water molecules, and 4 of the chloride ions. All polar hydrogen atoms have been included explicitly in the calculation, while those belonging to aliphatic and aromatic nonpolar groups have been treated according to the united atom approximation (Brooks et al., 1983). The empirical simple point charge (SPC) model for water molecules (Berendsen et al., 1981) has been used in the simulation. For dynamics integration, the Verlet algorithm (Verlet, 1967) with a time step of 1 fs has been used. All protein bond lengths were kept fixed by means of the SHAKE algorithm (Rickaert et al., 1977).

Potential function parametrization

The functional form of the potential employed is the same as for the CHARMM force field (Brooks et al., 1983). We used the united atom potential parameter set labeled CHARMM20. A group cutoff for electrostatic interactions of solute and solvent was employed. A nonbonded interaction spherical cutoff of 9.0 Å, smoothed by a cubic spline between 8 Å and the cutoff distance, was used.

Thermalization and trajectory computations

Before starting the thermalization a preliminary energy minimization of the protein-water system was obtained by using the conjugate gradient method implemented in the computer program MOIL (Elber et al., 1995). The MD simulation was performed in the microcanonical ensemble. At the beginning of the simulation the kinetic energy was set at 300 K by initializing the atomic velocities with a Maxwell-Boltzmann distribution. During equilibration the temperature was periodically rescaled. The total potential energy reaches a plateau after ~30 ps. We continued the equilibration for a further 30 ps to obtain conformations far enough from the initial crys-

tallographic conditions. After the equilibration we ran the system for a further 150 ps, collecting protein and solvent coordinates once every 50 fs. Since the motion of the lateral chain is of the order of 10^{-11}-10^{-10} s (McCammon and Harvey, 1987) we can conclude that, although a longer simulation time would be required for an exhaustive sampling and statistics, the present simulation has detected the main features of the lateral chains of the *Scapharca* dimer in solution.

Overall properties

To assess the reliability of the calculations and as a measure of structural stability, we performed a series of standard tests on the geometrical properties of *S. inaequivalvis* wild-type and mutant deoxy proteins. The stability checks were iteratively done running the DSSP program (Kabsch and Sander, 1983), which allows measurement during the entire trajectory: the total accessible surface area of the protein dimers, the number of residues in unfavorable regions of the Ramachandran plot corresponding to the number of residues in random coil conformation, the number of the backbone's hydrogen bonds, and the all-atom root mean square (r.m.s.) deviation from the minimized starting structure (Fig. 1). The r.m.s. deviation was computed removing global translations and rotations and optimally superimposing the instantaneous configurations on the starting one.

The total accessible surface of the two proteins stabilizes around an average value of 16,500 Å^2 (Fig. 1 *a*). The r.m.s. deviation from the reference structure is more stable in the mutant compared to the wild-type protein. This behavior indicates that the wild-type protein explores a number of conformations higher than the mutant protein (see Fig. 1 *e*). The other calculated properties remain quite stable during the simulation time (Fig. 1, *b*–*d*) and their stability could be considered as a clear indication of the maintenance of the original protein folding.

Optical spectroscopy

Samples

S. inaequivalvis Thr-72→Ile HbI mutant was obtained by site-directed mutagenesis on the HbI cDNA (Gambacurta et al., 1993). Expression was performed in *Escherichia coli* strain HB101 and the HbI mutant was obtained as a holoprotein and purified as previously described (Gambacurta et al., 1995).

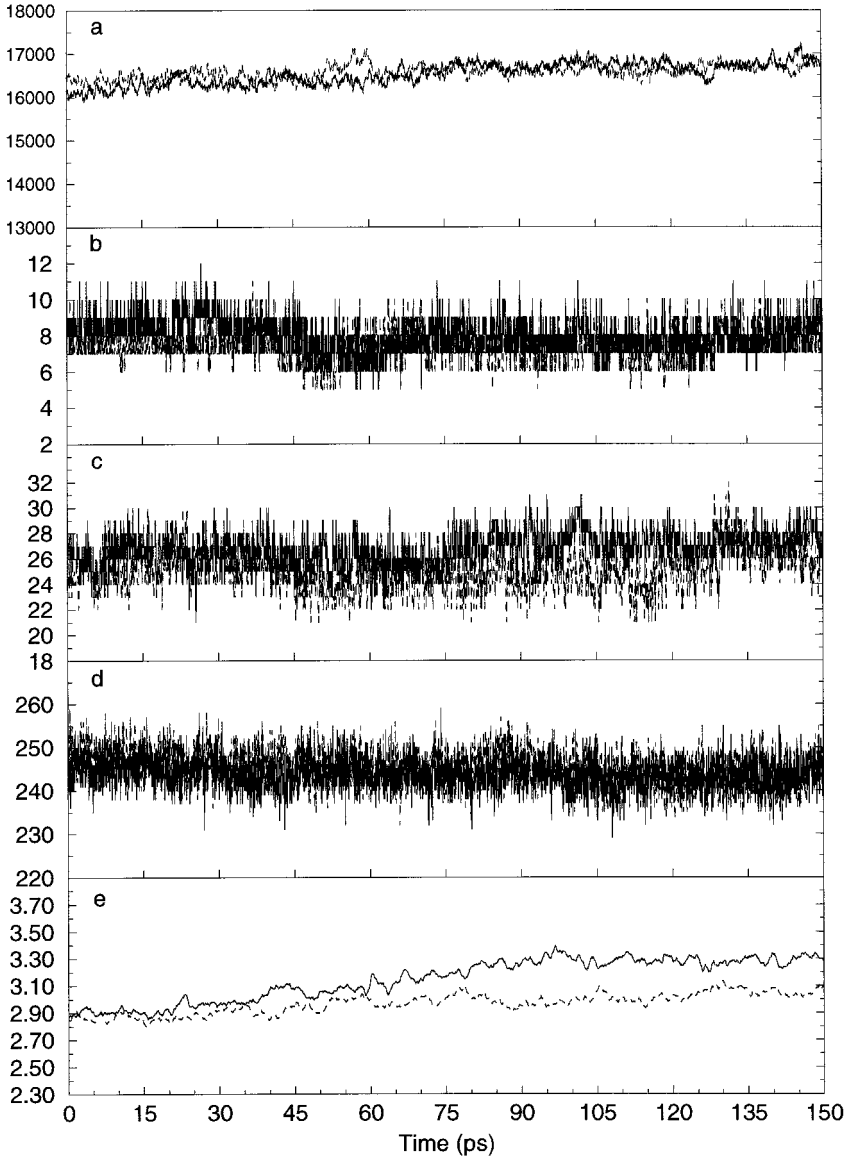

FIGURE 1 Geometrical properties of *S. inaequivalvis* deoxy wild type (——), and mutant (- - - - -) HbI. (*a*) Total accessible surface (Å^2). (*b*) Number of residues in unfavorable regions of the Ramachandran plot. (*c*) Number of residues in random coil conformation. (*d*) Number of backbone's hydrogen bonds. (*e*) All-atoms root mean square deviation from the minimized starting structure.

Samples for spectrophotometric measurements were prepared by diluting concentrated oxyhemoglobin stock solutions into a 65% (v/v) glycerol-buffer mixture (0.1 M phosphate buffer pH 7.0 in water at room temperature) to give a final concentration of ~10 μM in heme. For measurements on the CO and deoxy derivatives the above solutions were first equilibrated with 1 atm of CO and N_2, respectively. A small amount of sodium dithionite (to give a final concentration of $\sim 3 \cdot 10^{-4}$ M) was therefore anaerobically added to obtain fully reduced samples.

Soret band

Absorption spectra (500–370 nm) were measured on a Cary 2300 spectrophotometer (Varian Associates Inc., Palo Alto, CA) with a 0.5-nm bandwidth, 1-s time constant, 0.5 nm/s scan speed; they were digitized in intervals of 0.5 nm. The baseline (cuvette + glycerol + buffer) was measured at room temperature and subtracted from each spectrum; in fact, in the spectral range of interest the baseline does not depend on temperature, although at the concentrations used the absorption due to dithionite becomes relevant only at wavelengths <~370 nm. A detailed description of the theoretical approach used to obtain an analytical expression for the Soret band profile has been given previously (Cupane et al., 1995). Here we report only a brief summary.

The absorption lineshape is considered to arise from the convolution of three terms:

$$A(\nu) = L(\nu) \otimes G(\nu') \otimes P(\nu_0) \tag{1}$$

The first term, $L(\nu)$, is a sum of Lorentzians, which arises from the coupling of the (intrinsically Lorentzian) electronic transition with high frequency vibrational modes ($h\nu_i > k_B T$) of the matrix surrounding the chromophore. Making use of the so-called "standard assumptions" (Champion and Albrecht, 1982) this term can be expressed as

$$L(\nu) = M\nu \sum_{\{m_i\}} \left[\prod_i^{N_h} \frac{S_i^{m_i} e^{-s_i}}{m_i!} \right] \cdot \frac{\Gamma}{[\nu - \nu' - \sum_i^{N_h} m_i \nu_i]^2 + \Gamma^2} \tag{2}$$

where M is a constant proportional to the square of the electric dipole moment, and Γ is a damping factor related to the finite lifetime of the electronically excited state. The sum extends over all possible combinations of m_i vibrational excitations in the various high frequency vibrational modes i. The linear coupling strength is represented by S_i. The second term, $G(\nu')$, takes into account the coupling of the electronic transition with a "bath" of low frequency modes of the system. Within the so-called "short times approximation" (Chan and Page, 1983) it can be shown that such a coupling generates a Gaussian distribution of the fundamental frequency ν':

$$G(\nu') = \frac{1}{\sqrt{2\pi}\sigma} \exp[-\nu' - \nu_0]^2/2\sigma^2 \tag{3}$$

where σ is the width of the distribution

When the effects of coupling with both high and low frequency modes are taken into account, the spectral lineshape is therefore given by a superposition of Voigtians (convolutions of Lorentzians and Gaussians). The third term, $P(\nu_0)$, takes into account the inhomogeneous broadening of the Soret line that arises from conformational heterogeneity due to the presence of conformational substates (Frauenfelder et al., 1988; Ormos et al., 1990) and different heme group environments. Inhomogeneous broadening can be taken into account by assuming a distribution of the ν_0 frequency not dependent on temperature.

Modeling this distribution as a Gaussian curve yields formally perfect fits to the spectra of the CO derivative, but is not sufficient to describe the lineshape of the deoxy spectra (Srajer et al., 1986; Srajer and Champion, 1991; Cupane et al., 1993a, 1995). In the case of deoxy hemoproteins, regarding their out-of-plane displacement, the disorder in the position and orientation of the heme iron compared to the heme plane (Srajer et al., 1986; Srajer and Champion, 1991) contributes a non-Gaussian distribution of 0–0 transition frequencies. An analytical expression for this distribution has been developed (Srajer et al., 1986) in terms of a statistically distributed iron coordinate Q, Q_0 being the mean coordinate position and δ the width of the distribution:

$$P(\nu) = \frac{1}{2\delta\sqrt{(\nu - \nu_0)2\pi b}} \left[\exp\left(-\frac{[(\nu - \nu_0)^{1/2} + Q_0\sqrt{b}]^2}{2b\delta^2} \right) + \exp\left(-\frac{[(\nu - \nu_0)^{1/2} + Q_0\sqrt{b}]^2}{2b\delta^2} \right) \right] \tag{4}$$

Fittings of the measured spectra were performed with Eq. 1, using a Gaussian with halfwidth σ_{in} for the distribution $P(\nu_0)$ in the case of the CO derivative, and Eq. 4 in the case of the deoxy derivative. As usual (Di Pace et al., 1992; Cupane et al., 1993a, b), a Gaussian curve centered at 29,000 and 26,500 cm^{-1}, respectively, were added to the fits to take into account contributions from the N band. Fitting parameters were M, Γ, S_j, σ, ν_0, $Q_0\sqrt{b}$, and $\delta\sqrt{b}$. The last two parameters were used for the fitting of the deoxy derivative only. The ν_j values of the high frequency modes were taken from resonance Raman spectra (Bangcharoenpaurpong et al., 1984; Spiro, 1983; Morikis et al., 1991; Rousseau et al., 1993). Because the less-coupled modes do not contribute significantly to the observed spectra, only the most-coupled ones have been considered; namely 1) for the deoxy derivative: ν = 370 cm^{-1}, ν = 674 cm^{-1}, ν = 1357 cm^{-1}; 2) for the liganded derivatives: ν = 350 cm^{-1}, ν = 676 cm^{-1}, ν = 1374 cm^{-1}.

It should be pointed out that the modes at 370 cm^{-1} and 350 cm^{-1} in the deoxy and liganded derivatives, respectively, are average frequencies accounting for spectral regions characterized by several quasi-degenerate peaks. Indeed, we recall that a limit to our resolution of vibronic structure is posed by the intrinsic (homogeneous) width of the Soret band that, as shown by the values of parameter G reported in Table 1, is ~200 cm^{-1}: 674 (676) and 1357 (1374) cm^{-1} correspond to the well-known ν_7 and ν_4. However, in view of the above argument, contributions to S_{674} (S_{676}) coming from the coupling with the nearby modes at ~750 and 780 cm^{-1} cannot be excluded. Equal ν values have been used for native and mutant HbI.

Within the harmonic approximation, the temperature dependence of parameters σ and ν_0 can be expressed as

$$\sigma^2 = NSR^2\langle\nu\rangle^2 \coth(h\langle\nu\rangle/2kT) + \sigma_{in}^2 \tag{5}$$

$$\nu_0 = \nu_{00} - 1/4\, N\langle\nu\rangle(1 - R)\coth(h\langle\nu\rangle/2kT) + C \tag{6}$$

TABLE 1 Values of the parameters that characterize the coupling of the Soret band with low-frequency and high-frequency vibrational modes

Protein	$\langle\nu\rangle$	NS	σ_{in}	Γ	S_{370}*	S_{674}*	S_{1357}*	$Q_0\sqrt{b}$	$\delta\sqrt{b}$
HbI native	120 ± 10	0.6 ± 0.1	—	180 ± 5	0.05 ± 0.01	0.08 ± 0.01	0.06 ± 0.01	0.20 ± 0.02	0.16 ± 0.02
HbI mutant	170 ± 10	0.4 ± 0.1	—	215 ± 10	0.19 ± 0.03	0.20 ± 0.04	0.07 ± 0.01	0.12 ± 0.02	0.16 ± 0.02
HbICO native	208 ± 5	0.5 ± 0.1	0 ± 20	250 ± 5	<0.01	0.08 ± 0.01	0.09 ± 0.01	—	—
HbICO mutant	207 ± 10	0.5 ± 0.1	0 ± 20	245 ± 10	<0.01	0.11 ± 0.05	0.09 ± 0.01	—	—

*For the liganded derivatives the reported values refer to the modes at 350, 676, and 1374 cm^{-1}, respectively.

where $\langle\nu\rangle$, S, and R are the effective frequency, linear, and quadratic constants, respectively, of the low frequency bath; N is the number of soft modes, ν_{00} is the frequency of the purely electronic transition, and C takes into account other temperature-independent contributions to the peak position. The term σ^2_{in} in Eq. 5 arises from inhomogeneous broadening and is used only in the case of the CO derivative, because for the deoxy spectra this effect is taken into account by the parameter $\delta\sqrt{b}$.

Near-infrared band III

Absorption spectra in the near-infrared region (850–650 nm) were measured on a Cary 2300 spectrophotometer (Varian Associates Inc., Palo Alto, CA) with 1-nm bandwidth, 0.5-s time constant, 1 nm/s scan speed, and were digitized in intervals of 0.5 nm. For this experiment the protein concentration was 0.7 mM (in heme). The first moment M_1 of band III was calculated from the spectral profile after subtracting the tangent between the minima at each temperature, following exactly the same procedure reported by Huang et al., 1996.

The 20 K absorption spectrum of the photoproduct was measured after photolysis of a sample mutant HbI-CO, following the procedure described by Cordone et al., 1990.

Raman spectroscopy

Sample preparation

CO derivatives were prepared from an oxyhemoglobin stock solution by passing CO gas over the surface of a 100-μl aliquot in a sealed vial. Deoxy derivatives were prepared by passing N_2 over the sample and then adding five equivalents with respect to heme concentration of sodium dithionite. All samples were ~1 mM (in heme), 0.1 M potassium phosphate buffer, pH 7.0. The samples were then loaded in a nitrogen atmosphere into quartz sample cells with a 200-μm pathlength (Helma P/N 124-QS, Jamaica, NY). The front window of the cell was replaced with a sapphire window, which yielded a flatter baseline in the low frequency region of the Raman spectrum. The sample cell was mounted in a custom brass holder, which was cooled to ~10°C and rotated fast enough so that a new sample volume was interrogated with each laser shot. Photoproduct buildup and artifacts from sample spinning were found to be negligible by varying the spinning rate and by taking visible absorption spectra before and after each experiment. This sample preparation and arrangement was used for both the Raman and flash photolysis experiments.

Experimental apparatus

Visible time-resolved resonance Raman spectra were obtained using an 8-ns 435.8-nm pulse to both photodissociate the ligand and Raman scatter-off the sample. The laser used was a Nd:YAG laser (Continuum NY81C-20, Santa Clara, CA), which produced 450 mJ pulses at 20 Hz in the second harmonic output at 532 nm. Four watts of the 532-nm beam was focused into a homemade 90-cm long cell filled with 120 psi of hydrogen to Raman-shift the laser to 435.8 nm. Neutral density filters were used to reduce the energy of the 435.8-nm pulses to 150 μJ, and these were focused with a 150-mm plano-convex lens on the sample at an incidence angle of 45°. The Raman-scattered light was collected at normal incidence to the sample (135 to the laser) with a 50-mm Nikon F/1.4 camera lens and focused with an f-matching lens onto the 50-μm × 5-mm slit of a 0.64-m single monochromator utilizing an 1800 grooves/mm grating (ISA HR640, Metuchen, NJ). The Rayleigh line was reduced in intensity with a holographic notch filter that was angle-tuned to remove the scattered laser light (Kaiser P/N HNF-1171 centered at 442 nm at an incidence angle of 14°, Ann Arbor, MI). Intensity artifacts created by polarization-dependent grating reflectivity were eliminated with a depolarizer used to scramble the polarization of the collected light (CVI P/N DPL-10, Putnam, CT). The detector was an intensified diode array run in the cw mode (Princeton Instruments P/N IRY-1024S/B, Trenton, NJ). The total accumulation time per spectrum was typically 30 min. The spectral bandwidth of the monochromator was ~2.5 cm^{-1}, and the resolution of the detector array was ~0.9 cm^{-1} per pixel. Raman spectra were calibrated using solvent spectra with previously determined peak assignments. A least-squares-fit was used to map pixel numbers into relative wavenumbers (Raman shift). The Raman spectra were baselined using a polynomial fitting routine in LabCalc and are presented without smoothing (Galactic Industries, Salem, NH).

RESULTS AND DISCUSSION

Molecular dynamics

The averaged MD structures of the wild-type and mutant deoxy *S. inaequivalvis* HbI are similar, indicating that the deoxygenated mutant remains in the T state. However, a close analysis of the trajectories indicates a different behavior, mainly at the level of the residues, indicated by examinations of the x-ray structure of the protein, in the liganded and unliganded state, to play a determinant role in the CO or O_2 binding (Royer, 1994). In the Thr-72→Ile mutant the Ile-72 and Ile-71 of one subunit fluctuate at an interacting distance with Val-93′ of the other subunit, almost blocking this residue in a unique conformation and allowing a tight interaction between the E and F helices at the dimer interface. As an example, the fluctuations of the distance between Cδ1, Cγ1, and Cγ2 of Ile-71 and Cγ2 of Val-93′ are reported in Fig. 2 for the mutant and the native deoxy form. Such values are not completely identical in the two subunits because of an internal asymmetry, as already reported by Royer (1994); however, in both cases the contacts are closer in the mutant than in the wild-type protein. This interaction may be similar to that described upon binding of mercurial compounds to Cys-92 which, as in our case, results in an increase in oxygen affinity and loss of cooperativity (Furuta et al., 1980; Boffi et al., 1987). The closer Ile-72, Ile-71–Val-93′ contacts allow a small helix rearrangement and the consequent movement of the residues Phe-80′, Val-94′, Phe-11′, Val-142′, Leu-138′, Leu-146′, which create a small crevice under the heme pocket that may be occupied by Phe-97′ through a small rotation of its side chain toward the internal part of the protein. The movement of Phe-97′ in the deoxy mutant allows the carbonyl of Phe-97′ to fluctuate at a hydrogen bond distance with both the amide nitrogen and the Nδ1 of the proximal His-101′, while in the wild type the Phe-97′ carbonyl fluctuates at a hydrogen bond distance only with the Nδ1 of His-101′ (Fig. 3). In native HbI upon CO binding the side chain of Phe-97 is extruded toward the subunit interface and the backbone displacement makes the His-101 Nδ1–Phe-97 O hydrogen bond shorter than that observed in the deoxy structure (Royer et al., 1990). The shorter hydrogen bond is considered important to explain the oxygen affinity of the wild type (Royer et al., 1990), since binding of O_2 or CO causes a withdrawal of partial negative charge from the iron atom to the ligand, leaving a partial positive charge on the proximal histidine, which may be stabilized by hydrogen bonds (Caughey et al., 1975). In the Thr-72→Ile deoxy mutant the steric hindrance

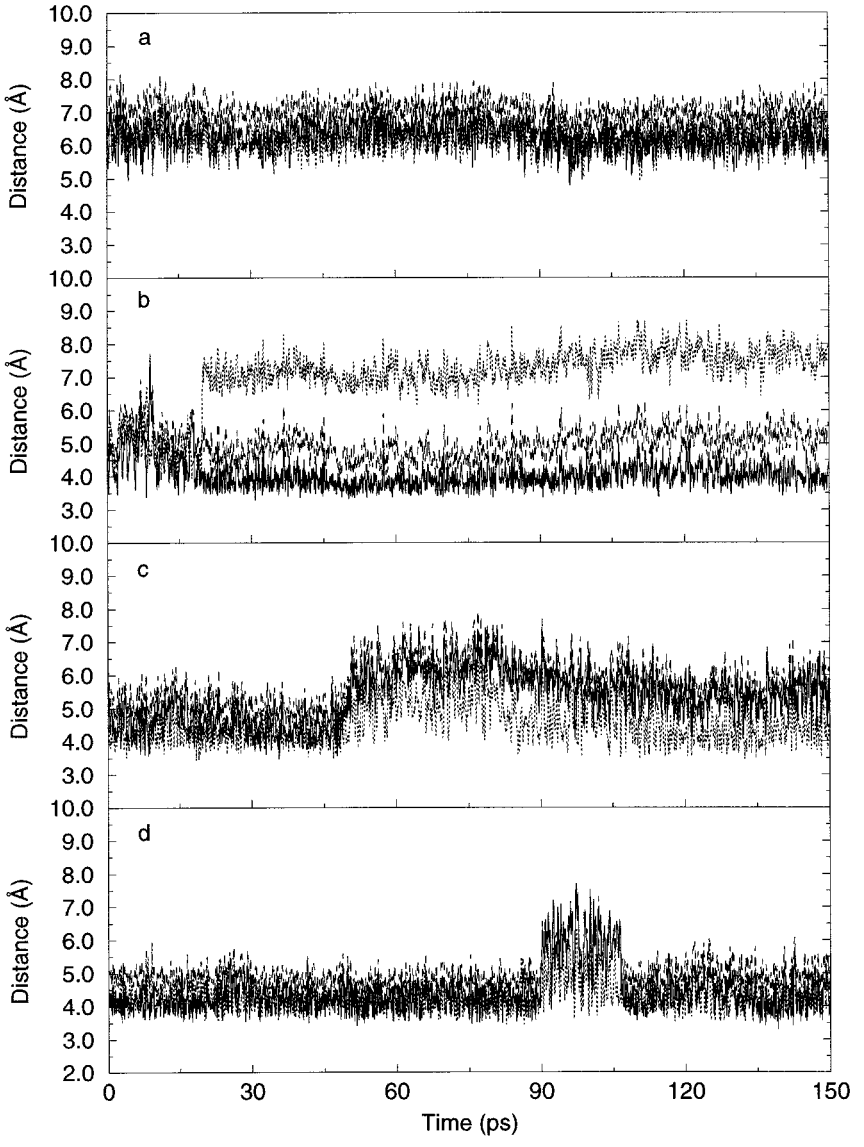

FIGURE 2 Trajectories of the *S. inaequivalvis* deoxy HbI intersubunit contacts between the side chains of Ile-71 and Val-93′. (*a*) Fluctuations of the distances between Cδ1, Cγ1, Cγ2 of Ile-71 of the A subunit, and Cγ2 Val-93 of the B subunit in the wild-type protein. (*b*) Fluctuations of the distances between Cδ1, Cγ1, Cγ2 of Ile-71 of the B subunit, and Cγ2 Val-93 of the A subunit in the wild-type protein. (*c*) Fluctuations of the distances between Cδ1, Cγ1, Cγ2 of Ile-71 of the A subunit, and Cγ2 Val-93 of the B subunit in the mutant protein. (*d*) Fluctuations of the distances between Cδ1, Cγ1, Cγ2 of Ile-71 of the B subunit, and Cγ2 Val-93 of the A subunit in the mutant protein. The distances are labeled by the following symbols: Cδ1 Ile-71–Cγ2 Val-93′ (——), Cγ1 Ile-71–Cγ2 Val-93′ (- - - - -), and Cγ2 Ile-71–Cγ2 Val-93′ (· · · ·).

of the lateral chain of Ile-72 induces rotation of Phe-97′ in the interior of the protein, with an additional hydrogen bond with the amide nitrogen of His-101, which may further stabilize a withdrawal of charge due to the O_2 or CO binding to the metal.

The MD simulation also indicates that in the deoxy mutant several protein residues shown to play a role in the ligand binding fluctuate around an orientation similar to that observed in the x-ray structure of native HbI-CO. Fig. 4 shows the trajectories corresponding to the O Lys-96–N Asn-100 distance for the deoxy mutant and the wild type in both subunits. As already mentioned, some asymmetry exists between the two subunits, so that a hydrogen bond is formed only in one subunit of the mutant. However, fluctuations around a regular and constant distance of ~4 Å are also observed in the other mutant subunit, at variance with that observed in the wild type, where such distance has large variations for both subunits (see Fig. 4). Accordingly, a hydrogen bond between these two residues occurs in the HbI-CO structure (Royer, 1994) and, together with the Phe-97–His-101 bond, makes the bend of the second part of the F helix more gentle, which is usually quite sharp in the wild-type deoxy protein, where these hydrogen bonds are lacking. Moreover, the number of water molecules that dynamically populate the dimer interface, calculated as the water molecules at a distance lower than 4.0 Å from both subunits, is lower for the mutant than for the native protein, suggesting that the heme pocket of the mutant feels, in average, an environment more hydrophobic than in the native HbI (Fig. 5).

Interesting changes are also observed at the level of Arg-53 and Arg-104. These two residues in the wild type fluctuate around a favorable distance to the hydrogen bond with the D and A propionate groups, respectively, over all the explored simulation time (Fig. 6), while such distances are much longer for the deoxy mutant. In agreement with these findings, the two structures described by Royer indicate optimal distances for hydrogen bonds in the deoxy, but

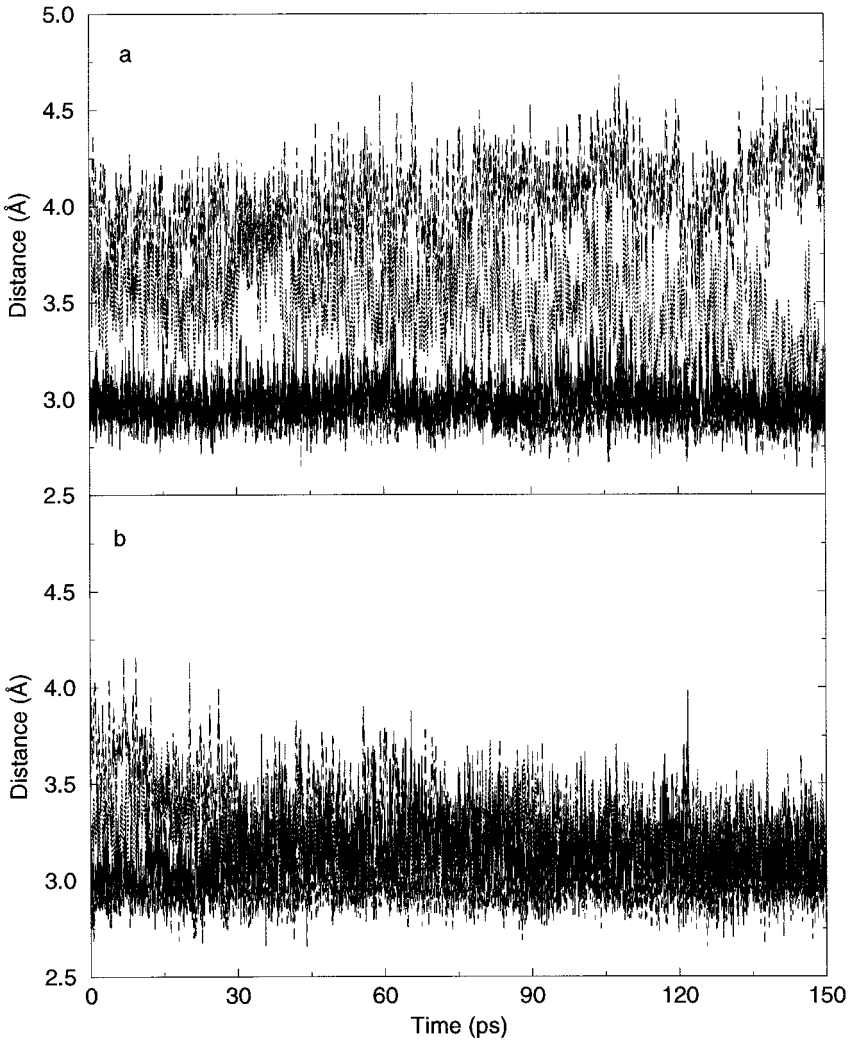

FIGURE 3 Trajectories of the *S. inaequivalvis* deoxy HbI intrasubunit O Phe-97–N His-101 (· · · · ·) and O Phe-97–Nδ1 His-101 (——) distance in subunit A, and O Phe-97–N His-101 (— - —) and O Phe-97–Nδ1 His-101 (- - - - -) distance in subunit B of the (*a*) wild-type and (*b*) mutant protein.

not in the HbI-CO, form. These differences may have a role in the information transfer between the two heme sites. Another interesting observation that may be correlated with the lower cooperativity of the mutant protein concerns the value of the calculated Debye-Waller factors ($8\pi^2/3 \cdot \langle(\Delta r)^2\rangle$) for the heme, which are lower in the mutant than in the native protein (Fig. 7). It may be guessed that a rigid heme is less prone to feel the intersubunit communications.

Optical spectroscopy

Fig. 8 shows the absorption spectra of deoxy and CO HbI mutant at various temperatures between 300 and 25 K. A fit of the 25 K spectrum in terms of Eq. 1 is reported in Fig. 9 for both forms of the protein. Values of the coupling constants to the high frequency modes and of parameter *G* obtained from the fittings are listed in Table 1, together with those previously observed for the wild type (Boffi et al., 1994). The deoxy mutant displays values of S_{370} and S_{674} higher than those relative to the deoxy native, indicating an higher coupling with these modes likely due to a slightly more planar (Cupane et al., 1996) heme geometry in the mutant.

The parameters reported in Table 1 also indicate a value of $Q_o\sqrt{b}$ for the mutant deoxy lower than that of the wild type (0.12 vs. 0.2), indicating a smaller asymmetry of the Soret band in the mutant. This finding is in agreement with the hypothesis that the deoxy mutant reaches a conformation that is more prone to bind the external ligand. Also, the parameter *G* is larger for the mutant, and its value (215 cm^{-1}) is shifted toward the values observed for the CO derivatives (Table 1).

The temperature dependence of the peak frequency (ν_0) and Gaussian width (σ^2) for the mutant protein in the deoxy and CO reacted form is reported in Figs. 10, *a* and *b* and 11, *a* and *b* in comparison with analogous data relative to the native protein (Boffi et al., 1994). These parameters do not follow the behavior predicted by the harmonic approximation (Eqs. 5 and 6) in the whole temperature range 25–300 K; this is particularly evident for σ^2 relative to the deoxy derivatives, since a straight line tangent to the high temperature experimental data would extrapolate at $T = 0$ to

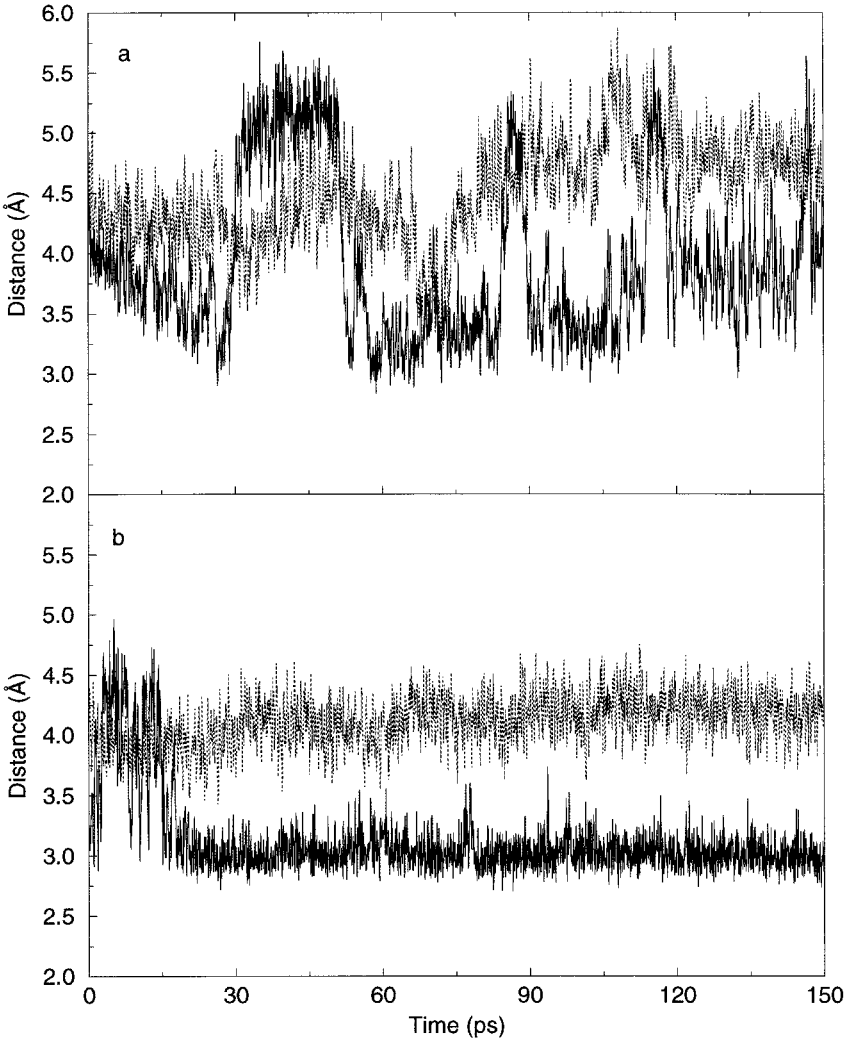

FIGURE 4 Fluctuations of the *S. inaequivalvis* deoxy HbI intrasubunit O Lys-96–N Asn-100 distance in the subunit A (——) and subunit B (· · · ·) of the (*a*) wild-type and (*b*) mutant protein.

negative values. A proper fit in terms of Eqs. 5 and 6 can be performed in the range 25–120 K (deoxy derivative) and 25–180 K (CO derivative); the continuous lines in Figs. 10 and 11 represent such fittings, and values of the parameters $\langle\nu\rangle$ and NS are reported in Table 1, in comparison with the analogous data relative to the native protein (Boffi et al., 1994). From Table 1 it can be seen that a larger value of $\langle\nu\rangle$ is observed for the deoxy mutant compared to the deoxy wild type, whereas a similar effect is not observed for the CO derivatives. This indicates that in the deoxy mutant derivative the heme is coupled to a more rigid environment than the native deoxy protein, in accordance with the MD simulations in which a larger rigidity of the protein around the heme group arises because of the occurrence of two hydrogen bonds between the carbonyl of Phe-97 and both the amide nitrogen and the Nδ1 of the proximal His-101. Lower Debye-Waller factors are also found mainly for the peripheral heme atoms (the propionates, see Fig. 7). The deviations of σ^2 values from the harmonic behavior observed (at temperatures higher than ~120 K and ~180 K) for the deoxy and CO mutant derivatives are analogous to those already reported for other hemoproteins (Di Pace et al., 1992; Cupane et al., 1995) and are attributed to the onset of nonharmonic nuclear motions. These anharmonic contributions ($\Delta\sigma^2$, i.e., the difference between the experimental σ^2 values and the continuous lines in Figs. 10, *a* and *b* and 11, *a* and *b* are reported in Figs. 10 *c* and 11 *c* and compared with the analogous quantities relative to the native protein.

From Figs. 10 and 11 it can be seen that in the mutant protein ν_0 and σ^2 display a "break" at ~180 K for both the deoxy and CO forms. In the native protein such a break is less pronounced and is observed in the deoxy derivative for both ν_0 and σ^2, while in the CO derivative it is observed only for ν_0 (Boffi et al., 1994). Moreover, the onset of small anharmonic contributions, almost absent in the CO native protein, is observed for the mutant CO derivative at temperatures higher than ~180 K; at difference, the extent of anharmonicity is almost equal for the deoxy derivatives. Since the "break" can be correlated to the glass transition of the solvent matrix (Cordone et al., 1988; Cupane et al., 1994, 1995; Leone et al., 1994), its extent may be taken as an indicator of the communication between the heme and the solvent. Figs. 10, *a* and *b* and 11, *a* and *b* indicate that the native deoxy protein is more sensitive to the solvent than

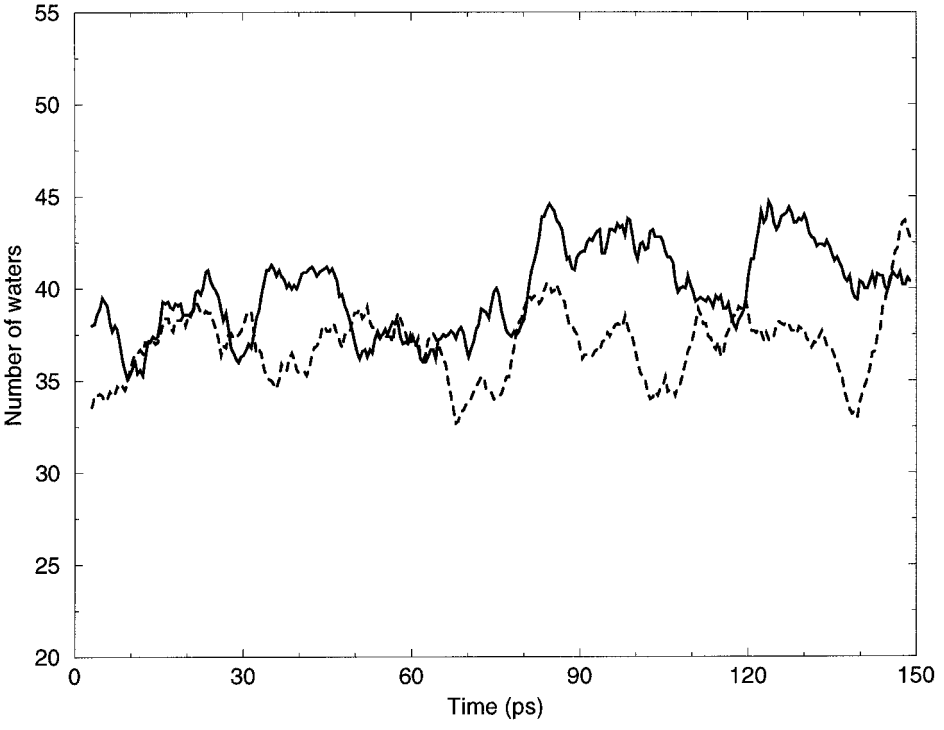

FIGURE 5 Time evolution of the number of water molecules populating the dimer interface of the wild-type (——) and mutant (· - · - ·) deoxy *S. inaequivalvis* HbI.

the CO derivative, in accordance with the x-ray structure, which indicates the presence of several more water molecules between the subunits in the deoxy than in the CO derivative because of the intersubunit location of Phe-97 upon ligand binding (Royer, 1994). However, the optical spectra also show that the mutant deoxy and CO derivatives have a similar communication with the solvent, in line with the MD calculations. These indicate a tight intersubunit interaction also in the deoxy form of the mutant, which may be correlated with the decreased cooperativity in ligand binding.

A further comment concerns the blue shift of ν_0 values observed for the mutant HbI compared to the wild type. In particular, for the deoxy derivative, such a blue shift increases sizeably upon lowering the temperature. In the low temperature photoproduct obtained by complete photolysis of sperm whale carbonmonoxy myoglobin, a red shift of the Soret band was observed and attributed mainly to a tilting of the proximal histidine away from the heme perpendicular (Srajer and Champion, 1991; Cupane et al., 1996); in analogy, one may interpret the blue shift observed in the mutant HbI as due to a more perpendicular position of the proximal histidine with respect to the heme plane. Moreover, an effect of the decreased polarity of heme environment in the mutant HbI on the peak position of the Soret band cannot be excluded. This interpretation is in line with the MD simulation data of Fig. 5, which indicate that the number of water molecules dynamically entering the interface space is lower in the mutant than in the wild-type HbI. Alternatively, the MD simulation does not underline any sizeable difference in the orientation of His-101 in the mutant in comparison with the native protein. The lack of a detectable difference in the MD trajectories may be due to the fact that a sizeable ν_0 blue shift is observed only at temperatures lower than ~200 K (see Fig. 10 *a*), while the MD simulation is carried out at 300 K.

Interesting structural information may also be worked out from the analysis of the "conformation sensitive" near-infrared band III, originating from a porphyrin-to-iron charge transfer transition. Fig. 12 *a* reports the bands of the native and mutant deoxy HbI at 300 K, while the thermal behavior of the first moments (M_1) in the temperature range 10–300 K is reported in Fig. 12 *b*. The band III of the mutant protein is broader and red-shifted with respect to the native one (Fig. 12 *a*; Huang et al., 1996). Band III of the native protein undergoes a blue shift upon lowering the temperature and its M_1 reaches a value of ~13,280 cm^{-1} (753 nm) at 10 K (Huang et al., 1996). A parallel blue shift is also observed for the mutant protein and the M_1 value at 20 K is ~13,170 cm^{-1} (759 nm). In the investigated temperature range (20–300 K), band III of the mutant protein is red-shifted by >100 cm^{-1} with respect to the native one at all temperatures. In Fig. 12 *b* the M_1 values observed for the photoproducts obtained by low temperature flash-photolysis of the CO derivatives are also reported (*triangles*). Both the native and the mutant proteins display an almost identical M_1 value of ~13,060 cm^{-1} (766 nm), indicating very similar local structures for the two photoproducts. Because at low temperatures structural relaxations are blocked, the spectrum of the 10 K photoproduct is assumed to correspond to the spectrum of the unrelaxed protein, and therefore to be diagnostic of the local conformation reached by the protein upon ligand binding. The 10 K spectrum of the equilibrium deoxy derivative of the mutant protein is more

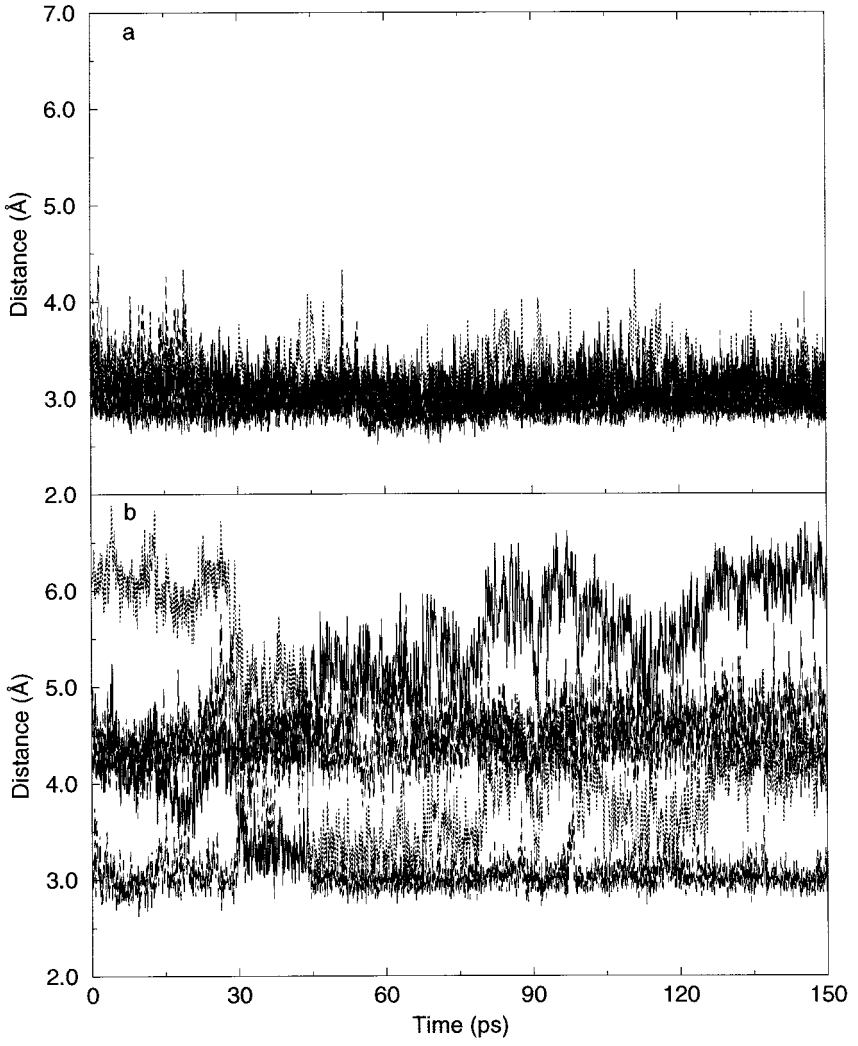

FIGURE 6 Fluctuations of the *S. inaequivalvis* deoxy HbI intrasubunit distances between Arg-53/Arg-104, and the heme propionates: Nϵ Arg-53 B–O1D Heme B (——), Nϵ Arg-53 B–O_2D Heme B (· · · ·), Nη2 Arg-53 B–O_2D Heme B (- - - - -), Nη2 Arg-104 B–O_2A Heme B (— - —), and Nη2 Arg-104 A–O_2A Heme A (— —); in the (*a*) wild-type and (*b*) mutant protein.

similar to that of the photoproduct than that of the native one, suggesting that there are conformational variables at the ligand binding site of the deoxy mutant that are more "R-like" than for the native protein.

Resonance Raman spectroscopy

Fig. 13 shows a comparison of the low frequency region of the resonance Raman spectrum for both the equilibrium and nonequilibrium five-coordinate ferrous forms of the wild-type and Thr-72→Ile mutant of HbI. The nonequilibrium species, designated Hb*(10 ns), is the photoproduct of the HbI-CO derivative within 10 ns from photodissociation.

The low frequency Raman spectrum of the deoxy derivative of the Thr-72→Ile mutant is very similar to that of the wild-type deoxy HbI, and does not show the changes associated with a transition to the higher-affinity R structures observed in both the photoproduct of the CO-bound ferrous derivative of HbI (Rousseau et al., 1993) and in the osmotically stressed deoxy derivative of HbI (Royer et al., 1996). The mutant shows a slight decrease in the frequency of the iron proximal histidine stretching bond ν (Fe-His), a slight decrease in the intensity of the 346 cm^{-1} band, and a slight broadening on the low frequency edge of the 371 cm^{-1} band. The slight decrease in the frequency ν (Fe-His) for the deoxy derivative of the Thr-72→Ile mutant is consistent with either a further weakening of the already weak hydrogen bond between the Nδ1 proton of the proximal histidine and the carbonyl of the Phe-97 residue or a conformational change that weakens the iron-proximal histidine bond. The molecular dynamics indicates that in the deoxy Thr-72→Ile mutant the phenyl ring of Phe-97 shifts further into the proximal heme pocket. This shift is opposite from the direction that Phe-97 moves upon ligand binding and could conceivably increase the repulsive interaction between the phenyl group and the proximal imidazole. Such an increase would be expected to lower the frequency of ν (Fe-His). Thus, the behavior of ν (Fe-His) in the deoxy derivative of the Thr-72→Ile mutant is consistent with the phenyl ring remaining in a T-state orientation with a possible slight shift that further increases proximal strain at the level of the iron-proximal histidine bond. Another possible explanation for the small decrease in the ν (Fe-His) frequency for the deoxy mutant compared to the deoxy wild type may be derived from the study of Sage et al. (1995), which suggests that a loss of water in the distal heme pocket of deoxy Mb results in a decrease in the ν (Fe-His) Raman frequency. These spectroscopic data are in agreement with the number of water molecules dynamically entering the dimer interface, which is lower in the mutant than in the native protein (Fig. 5). It is conceivable that the Thr-72→Ile mutation causes sufficient local disruption of the distal heme pocket environment to slightly change the occupancy of the water in the distal pocket, but does not cause a sufficient disruption of the interfacial water network to cause a transition toward the R quaternary state and the substantial increase in frequency observed at high (~90% v/v) glycerol concentrations (Royer et al., 1996).

The mutation-induced changes seen in the propionate-sensitive bands (346 and 371 cm^{-1}) are small enough to conclude that there is no quaternary structure change occurring for the deoxy mutant. However, they are

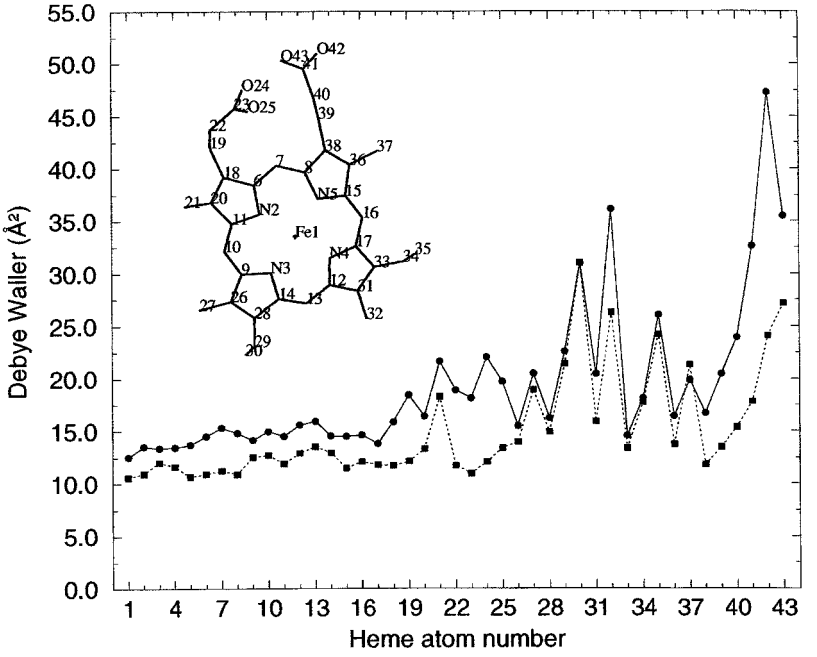

FIGURE 7 Averaged Debye-Waller factors for each heme atom of the wild-type (●), and mutant (■) deoxy *S. inaequivalvis* HbI. In the upper left of the picture is shown a scheme of the heme group where each atom is identified by a number. All the heteroatoms are explicitly labeled.

consistent with a small perturbation of the interface that is in the direction of the T-to-R transition.

The spectra of Hb*(10 ns) for both the wild type and the mutant show the characteristic changes relative to the deoxy Hb spectra that have been described previously (Rousseau et al., 1993). In particular, in going from the deoxy to the photoproduct spectra, there is an increase of several wavenumbers in the frequency of ν (Fe-His), a decrease in the intensity of the 346 cm^{-1} band, and a shift in the 371 cm^{-1} band down to 364 cm^{-1}. These changes have been ascribed to the R-state conformation formed via tertiary/quaternary structure changes associated upon ligand binding. Similar changes have also been reported for deoxy HbI subjected to osmotic stress through the addition of glycerol (Royer et al., 1996). The Hb*(10 ns) spectra of the wild-type and mutant are virtually identical, with the exception of the ν (Fe-His) band. The mutant exhibits a ν (Fe-His) band that is ~4 cm^{-1} higher in frequency than for the wild type. Nanosecond time-resolved Raman (Rousseau et al., 1993) and near-IR absorption (Huang et al., 1996) studies show that in the wild-type protein the relaxation upon photodissociation of the CO-bound derivative to the equilibrium deoxy T structure takes place within a few microseconds. Consequently, the spectrum of the photoproduct at 10 ns, Hb*(10 ns), is expected to reflect a conformation that closely approximates the initial conformation of the starting ligand bound species. The ν (Fe-His) frequency in the Thr-72→Ile

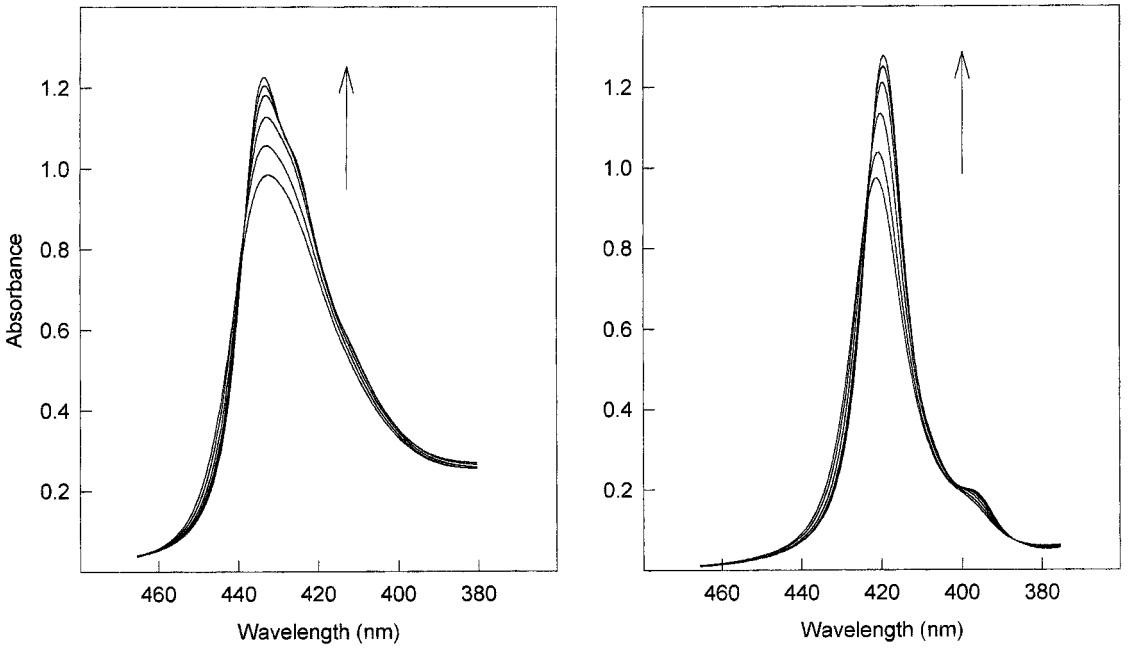

FIGURE 8 Optical absorption spectra (Soret band) of deoxy (*left panel*) and CO-bound (*right panel*) *S. inaequivalvis* mutant HbI at various temperatures between 300 and 25 K. The arrows in the figure indicate the direction of spectral changes observed upon lowering the temperature.

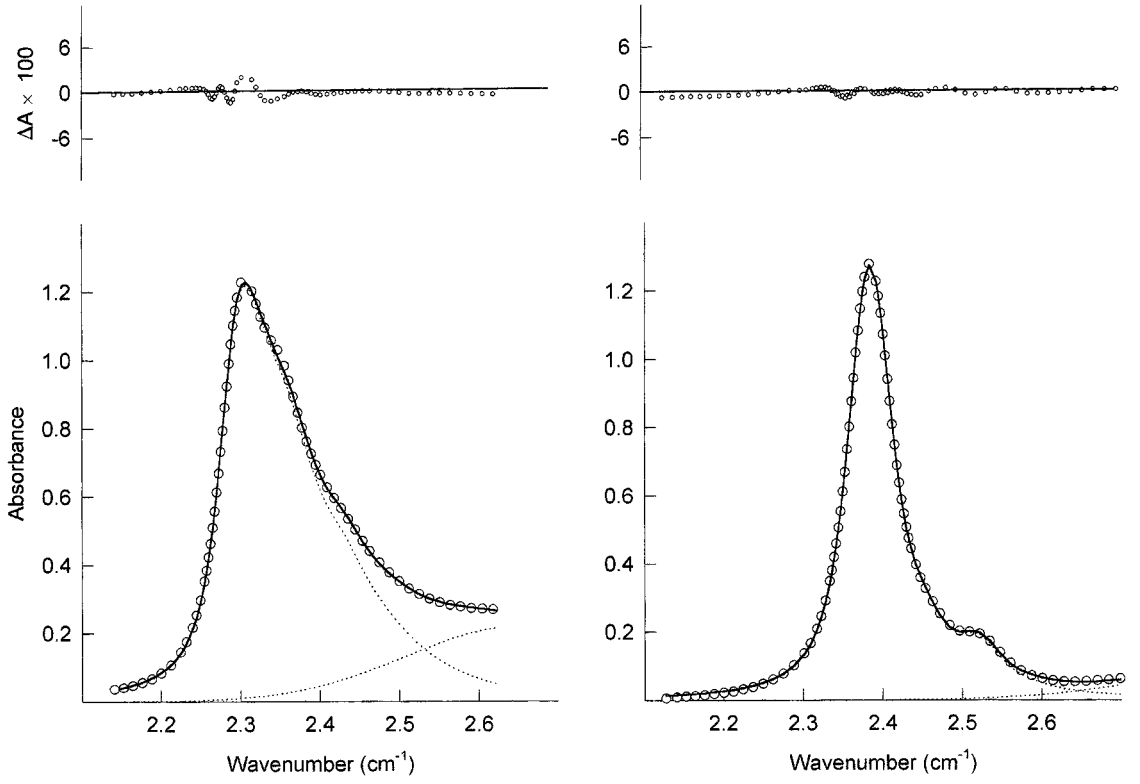

FIGURE 9 Deconvolution of the 25 K spectra in terms of Eq. 1. *Left panel:* deoxy derivative; *right panel:* CO derivative. Circles are the experimental points; dotted lines represent the theoretical Soret band profile and the high frequency Gaussian extrapolation (N band); the continuous line is the overall calculated spectral profile. For the sake of clarity, not all the measured experimental points are reported. The residuals are shown in the upper panels, on an expanded scale.

mutant Hb*(10 ns) spectrum indicates that the R state in the mutant contains less proximal strain than is present in the wild type.

The increase in the Thr-72→Ile ν(Fe-His) Hb*(10 ns) frequency could arise from a subnanosecond relaxation associated with HbI* that is slowed in the mutant. Support for this hypothesis comes from a preliminary measurement of the ligand rebinding times subsequent to photodissociation of HbI-CO using a 10-ns photodissociation pulse (Friedman, unpublished results). It is observed that for the wild type, the bimolecular ligand rebinding phase on the microsecond time scale and longer follows the anticipated slow T state kinetics, whereas for the Thr-72→Ile mutant this phase is substantially faster. This result is consistent with a considerable decrease in the relaxation rate of the R-state photoproduct to the T-state deoxy species. Conceivably, if there is a fast subnanosecond component associated with the relaxation of Hb*, it would also be slowed in the mutant. Picosecond and nanosecond time-resolved Raman experiments are planned to ascertain whether there is a fast subnanosecond relaxation, and whether the R-to-T relaxation is slowed for the mutant, as would be anticipated if the mutation stabilizes the R structure.

Despite the fact that the Hb*(10 ns) Raman spectrum indicates the stability of the R-state structure in the Thr-72→Ile has been enhanced, the Raman spectra also indicate that the deoxy derivative of the mutant remains in a T state conformation. In contrast, the shift of band III toward lower energy by >100 cm^{-1} (as well as data on the Soret band) would be suggestive of a more substantial shift toward the R state conformation for the deoxy derivative. A possible explanation for this quantitative discrepancy between spectroscopic markers is that band III has been shown to be responsive to electrostatic and hydrophobic effects (Kiger et al., 1995; Christian et al., 1997). Typically a less polar or more hydrophobic heme environment is associated with a shift of band III toward longer wavelengths. The partial loss of water from the T-state interface with a resulting decrease in the polarity of the distal heme pocket in the Thr-72→Ile mutant may be responsible for the shift of band III and the breakdown in its correlation with ν(Fe-His). Christian and Champion (Christian et al., 1997) have shown that loss of water from the heme pocket of deoxymyoglobin results in a small decrease in the frequency of the iron-proximal histidine-stretching frequency. Thus, it is also possible that the decrease in the frequency of this Raman mode for the deoxy *Scapharca* mutant might originate from a decrease in the occupancy of the heme pocket for water, as also suggested by the MD simulation (Fig. 5).

Another possibility arises from the different solvent conditions of the resonance Raman (in phosphate buffer) and optical absorption spectroscopy (phosphate buffer + 65% glycerol) experiments. In fact, it is known that in the deoxy HbI the addition of high concentrations (~90%) of glycerol causes a shift toward the R conformation (Royer et al., 1996). It is possible that the deoxy Thr-72→Ile mutant is more sensitive to the above-mentioned glycerol effect than the native deoxy protein, thus explaining the enhanced R-state stabilization detected by optical absorption spectroscopy.

CONCLUSIONS

The results obtained from both the MD simulations and the spectroscopic experiments indicate that the higher ligand affinity displayed by the Thr-72→Ile *S. inaequivalvis* HbI mutant is mainly due to local changes in the dimer interface and at the hemes that partially destabilize the T state and stabilize R state.

The low frequency Raman spectrum of the mutant equilibrium deoxy derivative shows a slight decrease of ν (Fe-

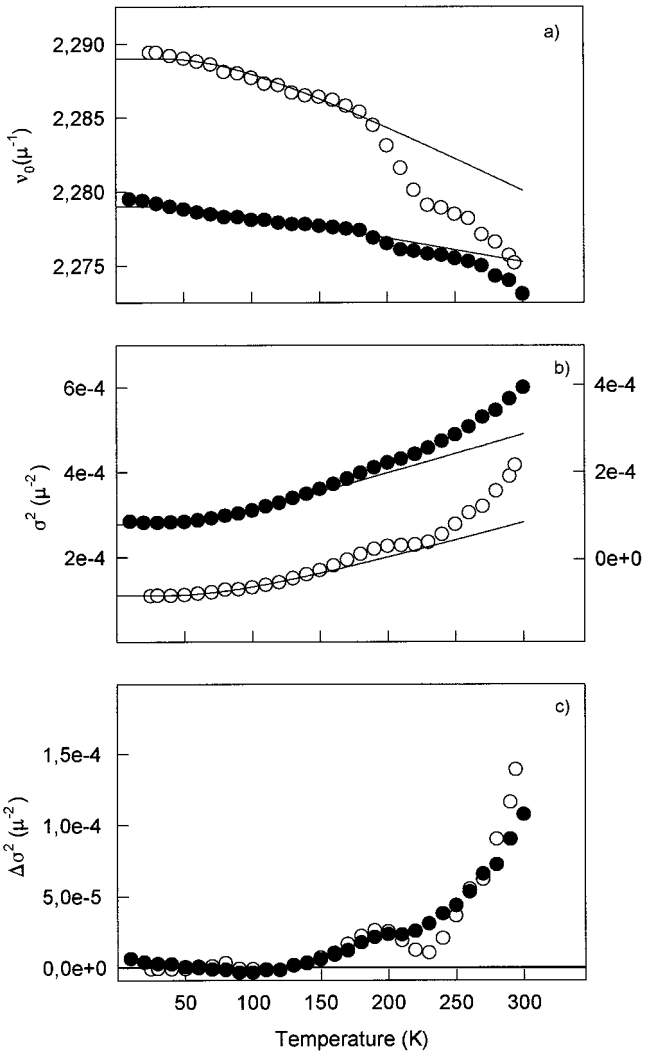

FIGURE 10 Temperature dependence of parameters: ν_0 (*a*), σ^2 (*b*), and $\Delta\sigma^2$ (*c*) for the deoxy derivatives. Filled symbols refer to native HbI (data taken from Boffi et al., 1994), open symbols refer to the mutant HbI. For the sake of clarity, σ^2 values relative to the native protein have been shifted upward [scale to the right of (*b*)]. Continuous lines represent fittings of the low temperature data in terms of Eqs. 5 and 6.

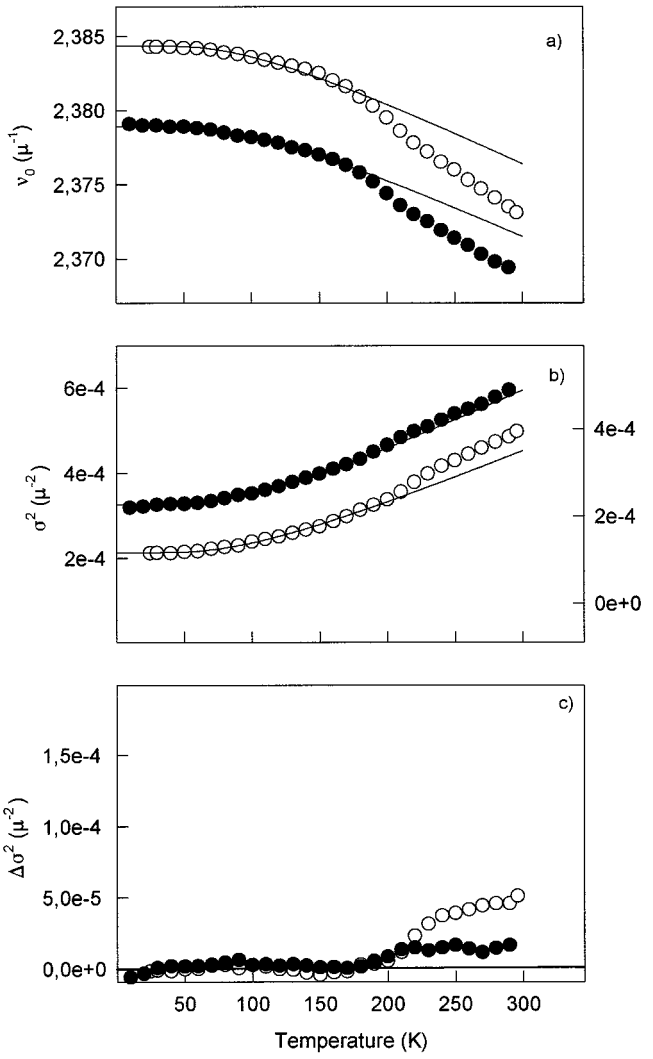

FIGURE 11 Same as in Fig. 10, for the CO derivatives.

His) that is consistent with either a further rotation of the phenyl ring toward the interior of the protein or a loss of water in the heme pocket (Christian et al., 1997). The mutation-induced changes in the propionate sensitive bands are consistent with a small perturbation at the subunit interface in the direction of the T-to-R transition. The room-temperature low frequency Raman spectrum of the 10-ns photoproduct of HbI-CO is consistent with a slowing down of the relaxation of the R-state photoproduct to the T-state in the mutant relative to the native protein.

The low temperature optical absorption spectra suggest that in the mutant deoxy derivative the Soret band is less asymmetric and the heme is more planar, while the mutant deoxy and CO derivatives have a similar communication with the solvent. The larger value of $\langle\nu\rangle$ observed with optical absorption spectroscopy in the mutant with respect to the native protein is indicative of a coupling of the heme to a more rigid environment. The red shift of the conformation-sensitive band III by >100 cm^{-1}, observed in the mutant, is consistent with a less polar or more hydrophobic heme environment and with a conformation wishing to switch toward an R state.

In agreement with these spectroscopic data, the MD results indicate that the heme environment assumes a higher rigidity in the mutant protein and that the number of water molecules entering the dimer interface is lower in the mutant than in the native protein. At the mean time the two subunits make closer contacts, and distances between specific residues, such as Lys-96–Asn-100, Arg-53–Arg-104, which have been shown to play a determinant role in the CO or O_2 binding, fluctuate around values similar to those observed in the ligand-bound structure of the native protein.

This work was supported in part by the Italian National Research Council (C.N.R.), the Italian Ministry of Scientific Research (M.U.R.S.T.), the W. M. Keck Foundation, and National Institutes of Health Grants

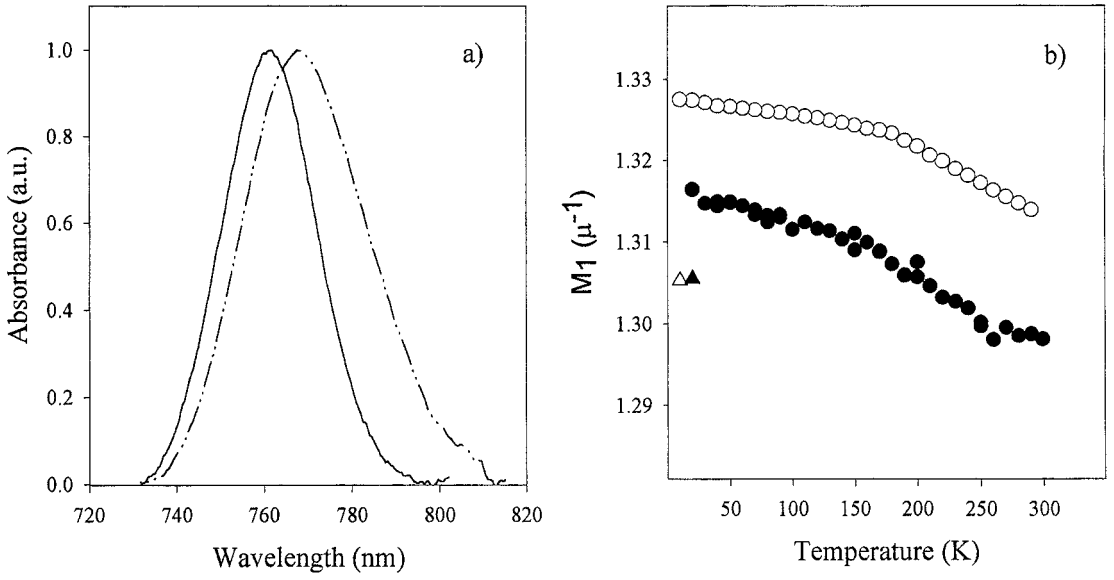

FIGURE 12 (*a*) Band III of native (*continuous line*) and mutant (*dashed line*) deoxy HbI at 300 K. The tangent between the minima has been subtracted from the experimental spectra before intensity normalization. (*b*) Temperature dependence of the first moment of the band. *Open symbols:* native HbI; *filled symbols:* mutant HbI. *Circles:* equilibrium deoxy derivatives; *triangles:* photoproducts obtained from flash-photolysis of the CO-derivatives. Data relative to the native protein have been taken from Huang et al., 1996.

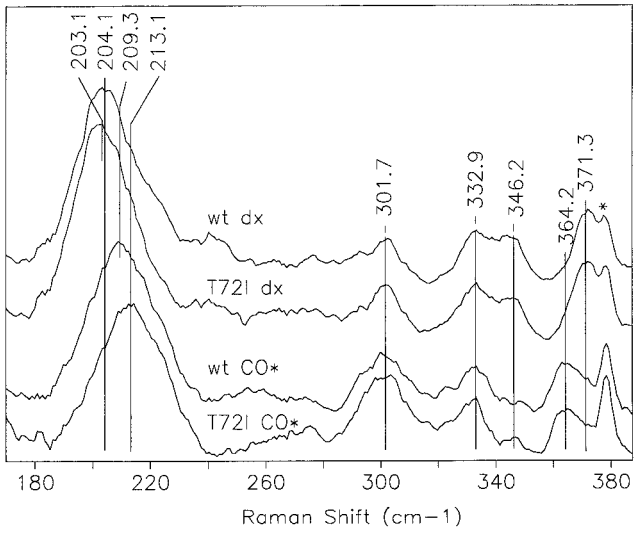

FIGURE 13 Low frequency resonance Raman spectra of equilibrium deoxy HbI wild type (curve"wt dx"), of equilibrium deoxy Thr-72→Ile mutant (curve "T72I dx"), of the 10 ns photoproduct of HbI-CO wild type (curve "wt CO*"), and of the 10 ns photoproduct of Thr-72→Ile HbI-CO mutant (curve "T72I CO*"). The spectral feature at ~380 cm^{-1}, marked with the asterisk, is from the sapphire window. For all the spectra the temperature is 283 K and the solvent is 0.1 M phosphate buffer pH 7.0.

R01GM44343, RO1HL58247, and PO1HL51084 (to J.M.F.). M. F. was an I.N.F.M. fellowship holder.

REFERENCES

Bangcharoenpaurpong, O., K. T. Schomacker, and P. M. Champion. 1984. A resonance Raman investigation of myoglobin and hemoglobin. *J. Am. Chem. Soc.* 106:5688–5698.

Berendsen, H. J. C., J. P. M. Postma, W. F. Van Gunsteren, and J. Hermans. 1981. Interaction models for water in relation to protein hydration. *In* Intermolecular Forces. B. Pullman, editor. Reidel, Dordrecht. 331–342.

Bernstein, F., T. Koetzle, G. Williams, E. Meyer Jr., M. Brice, J. Rodgers, O. Kennard, T. Shimanouchi, and M. Tasumi. 1977. The protein data bank: a computer based archival file for macromolecular structures. *J. Mol. Biol.* 112:535–542.

Boffi, A., M. Gattoni, R. Santucci, P. Vecchini, F. Ascoli, and E. Chiancone. 1987. Structural and functional effec s of selective chemical modifications of *Scapharca inaequivalvis* hemoglobins in relation to their unique assembly. *Biochem. J.* 241:499–504.

Boffi, A., D. Verzili, E. Chiancone, M. Leone, A. Cupane, V. Militello, E. Vitrano, L. Cordone, W. Yu, and E. E. Di Iorio. 1994. Stereodynamic properties of the cooperative homodimeric *S. inaequivalvis* hemoglobin studied through optical absorption spectroscopy and ligand rebinding kinetics. *Biophys. J.* 67:1713–1723.

Brooks, B. R., R. E. Bruccoleri, B. D. Olafson, D. J. States, S. Swaminathan, and M. Karplus. 1983. CHARMM: a program for macromolecular energy, minimization and dynamics calculations. *J. Comp. Chem.* 4:187–217.

Caughey, W. S., C. H. Barlow, J. C. Maxwell, J. A. Volpe, and W. J. Wallace. 1975. Reactions of oxygen with hemoglobin, cytochrome c oxidase and other hemeproteins. *Ann. N.Y. Acad. Sci.* 244:1–9.

Champion, P. M., and A. C. Albrecht. 1982. Resonance Raman scattering: the multimode problem and transform methods. *Annu. Rev. Phys. Chem.* 33:353–376.

Chan, C. K., and J. B. Page. 1983. Temperature effects in the time correlator theory of resonance Raman scattering. *J. Chem. Phys.* 79: 5234–5250.

Chavez, M., H. Courtney, M. Chance, D. Kiula, J. Nocek, B. Hofman, J. Friedman, and M. Ondrias. 1990. Structural and functional significance of inhomogeneous line broadening of band III in hemoglobin and Fe-Mn hybrid hemoglobins. *Biochemistry*. 29:4844–4852.

Chiancone, E., P. Vecchini, D. Verzili, F. Ascoli, and E. Antonini. 1981. Dimeric and tetrameric hemoglobins from the mollusk *Scapharca inaequivalvis. J. Mol. Biol.* 152:577–592.

Christian, J. F., M. Unno, J. T Sage, P. M. Champion, E. Chien, and S. G. Sligar. 1997. Spectroscopic effects of polarity and hydration in the distal heme pocket of deoxymyoglobin. *Biochemistry*. 36:11198–11204.

Cordone, L., A. Cupane, M. Leone, and E. Vitrano. 1990. Thermal behavior of the 760 nm absorption band in photodissociated sperm whale carbonmonoxymyoglobin at cryogenic temperature: dependence on external medium. *Biopolymers*. 29:639–643.

Cordone, L., A. Cupane, M. Leone, E. Vitrano, and D. Bulone. 1988. Interaction between external medium and heme pocket in myoglobin probed by low-temperature optical spectroscopy. *J. Mol. Biol.* 199: 213–218.

Cupane, A., M. Leone, V. Militello, M. E. Stroppolo, F. Polticelli, and A. Desideri. 1994. Low temperature optical spectroscopy of native and azide-reacted bovine Cu, Zn superoxide dismutase: a structural dynamics study. *Biochemistry*. 33:15103–15109.

Cupane, A., M. Leone, and E. Vitrano. 1993a. Protein dynamics: conformational disorder, vibrational coupling and anharmonicity in deoxyhemoglobin and myoglobin. *Eur. Biophys. J.* 21:385–391.

Cupane, A., M. Leone, E. Vitrano, and L. Cordone. 1995. Low temperature optical spectroscopy as a tool to study structure-dynamics-function relationships in heme proteins. *Eur. Biophys. J.* 23:385–398.

Cupane, A., M. Leone, E. Vitrano, L. Cordone, U. R. Hiltpold, K. H. Winterhalter, W. Yu, and E. E. Di Iorio. 1993b. Structure-dynamics-function relationships in Asian Elephant (*Elephas maximus*) myoglobin. An optical and flash-photolysis study on functionally important motions. *Biophys. J.* 65:2461–2472.

Cupane, A., E. Vitrano, G. U. Nienhaus, and P. Ormos. 1996. Heme geometry in the 10 K photoproduct from sperm whale carbonmonoxymyoglobin. *Biophys. Chem.* 60:111–117.

Dagget, V., and M. Levitt. 1993. Realistic simulation of native protein dynamics in solution and beyond. *Annu. Rev. Biophys. Biomol. Struct.* 22:353–380.

Di Pace, A., A. Cupane, M. Leone, E. Vitrano, and L. Cordone. 1992. Vibrational coupling, spectral broadening mechanisms, and anharmonicity effects in carbonmonoxy heme proteins studied by the temperature dependence of the Soret band lineshape. *Biophys. J.* 63:475–484.

Elber, R., A. Roitberg, C. Simmerling, R. Goldstein, H. Li, G. Verkhiver, C. Keasar, J. Zhang, and A. Ulitsky. 1995. Moil: a program for simulations of macromolecules. *Computer Phys. Commun.* 91:159–189.

Frauenfelder, H., F. Parak, and R. D. Young. 1988. Conformational substates in proteins. *Annu. Rev. Biophys. Biophys. Chem.* 17:451–479.

Furuta, H., M. Ohe, and A. Kajita. 1980. Ligand-dependent allosteric transformation of hemoglobins from the blood clam *Anadara broughtonii. Biochim. Biophys. Acta*. 625:318–327.

Gambacurta, A., M. C. Piro, and F. Ascoli. 1993. Cooperative homodimeric hemoglobin from *Scapharca inaequivalvis*. cDna cloning and expression of the fully functional protein in *E. coli*. *FEBS Lett.* 330:90–94.

Gambacurta, A., M. C. Piro, M. Coletta, M. E. Clementi, F. Polizio, A. Desideri, R. Santucci, and F. Ascoli. 1995. A single mutation (Thr-72→Ile) at the subunit interface is crucial for the functional properties of the homodimeric cooperative hemoglobin from *Scapharca inaequivalvis. J. Mol. Biol.* 248:910–917.

Gilch, H. R., R. Schweitzer-Stenner, W. Dreybrodt, M. Leone, A. Cupane, and L. Cordone. 1996. Conformational substates of the Fe2+-HisF8 linkage in deoxy myoglobin and hemoglobin probed in parallel by the Raman band of the ν (Fe-His) stretching vibration and the near-infrared band III. *Intl. J. Quantum Chem.* 59:301–313.

Huang, J., M. Leone, A. Boffi, J. M. Friedman, and E. Chiancone. 1996. Near-infrared spectra of *Scapharca* homodimeric hemoglobin: characterization of the deoxy and photodissociated derivatives. *Biophys. J.* 70:2924–2929.

Ikeda-Saito, M., T. Yonetani, E. Chiancone, F. Ascoli, D. Verzili, and E. Antonini. 1983. Thermodynamic properties of oxygen equilibria of dimeric and tetrameric hemoglobins from *Scapharca inaequivalvis. J. Mol. Biol.* 170:1009–1018.

Kabsch, W., and C. Sander. 1983. Dictionary of protein secondary structure: pattern recognition of hydrogen-bonded and geometrical features. *Biopolymers*. 22:2577–2637.

Kiger, L., F. Stetzkowsky-Marden, C. Poyart, and M. C. Marden. 1995. Correlation of carbon monoxide association rates and the position of absorption band III in hemoproteins. *Eur. J. Biochem.* 228:665–668.

Kuczera, K., J. Kuriyan, and M. Karplus. 1990. Temperature dependence of the structure and dynamics of myoglobin: a simulation approach. *J. Mol. Biol.* 213:351–373.

Leone, M., A. Cupane, V. Militello, and L. Cordone. 1994. Thermal broadening of the Soret band in heme complexes and in heme-proteins: role of the iron dynamics. *Eur. Biophys. J.* 23:349–352.

McCammon, J. A., and S. C. Harvey. 1987. *In* Dynamics of Proteins and Nucleic Acids. Cambridge University Press, London. 1987:66–71.

Melchers, B., E. W. Knapp, F. Parak, L. Cordone, A. Cupane, and M. Leone. 1996. Structural fluctuations of myoglobin from normal modes: Mössbauer-, Raman-, and absorption-spectroscopy. *Biophys. J.* 70: 2092–2099.

Morikis, D., P. Li, O. Bangcharoenpaurpong, J. T. Sage, and P. M. Champion. 1991. Resonance Raman scattering as a probe of electron-nuclear coupling: applications to heme proteins. *J. Phys. Chem.* 95: 3391–3398.

Ormos, P., A. Ansari, D. Braunstein, B. R. Cowen, H. Frauenfelder, M. K. Hong, I. E. T. Iben, T. B. Sauke, P. Steinbach, and R. D. Young. 1990. Inhomogeneous broadening in spectral bands of carbonmonoxymyoglobin: the connection between spectral and functional heterogeneity. *Biophys. J.* 57:191–199.

Procacci, P., T. A. Darden, E. Paci, and M. Marchi. 1997. ORAC: a molecular dynamics program to simulate complex molecular systems with realistic electrostatic interactions. *J. Comp. Chem.* 18:1848–1862.

Rickaert, J. P., G. Ciccotti, and H. J. C. Berendsen. 1977. Numerical integration of the Cartesian equations of motion of a system with constraints: molecular dynamics of N-alkanes. *J. Comp. Phys.* 23: 327–341.

Rousseau, D. L., S. Song, J. M. Friedman, A. Boffi, and E. Chiancone. 1993. Heme-heme interaction in a homodimeric cooperative hemoglobin: evidence from transient Raman scattering. *J. Biol. Chem.* 268:5719–5723.

Royer, W. E., Jr. 1994. High-resolution crystallographic analysis of a cooperative dimeric hemoglobin. *J. Mol. Biol.* 235:657–681.

Royer, W. E., Jr., W. A. Hendrickson, and E. Chiancone. 1990. Structural transitions upon ligand binding in a cooperative dimeric hemoglobin. *Science*. 249:518–521.

Royer, W. E., Jr., A. Pardanani, Q. H. Gibson, E. S. Peterson, and J. M. Friedman. 1996. Ordered water molecules as key allosteric mediators in a cooperative dimeric hemoglobin. *Proc. Natl. Acad. Sci. USA*. 93: 14256–14531.

Sage, J. T., K. T. Schomacker, and P. M. Champion. 1995. Solvent-dependent structure and dynamics in myoglobin. *J. Phys. Chem.* 99: 3394–3405.

Sassaroli, M., and D. L. Rousseau. 1987. Time dependence of the near-infrared spectra of photodissociated hemoglobin and myoglobin. *Biochemistry*. 26:3092–3097.

Song, S., A. Boffi, E. Chiancone, and D. L. Rousseau. 1993. Protein-heme interactions in hemoglobin from the mollusk *Scapharca inaequivalvis*. Evidence from resonance Raman scattering. *Biochemistry*. 32: 6330–6336.

Spiro, T. G. 1983. *In* Iron Porphyrins, Vol. II. A. B. P. Lever and H. B. Gray, editors. Addison-Wesley Publishing Co., Reading, MA. 89–159.

Srajer, V., and P. M. Champion. 1991. Investigations of optical lineshapes and kinetic hole burning in myoglobin. *Biochemistry*. 30:7390–7402.

Srajer, V., K. T. Schomacker, and P. M. Champion. 1986. Spectral broadening in biomolecules. *Phys. Rev. Lett.* 57:1267–1270.

Verlet, L. 1967. Computer "experiments" on classical fluids. I. Thermodynamical properties of Lennard-Jones molecules. *Phys. Rev.* 159: 98–103.